BBA
Biomembranes

Effects of a synthetic antitumoral catechin and its tyrosinase-processed product on the structural properties of phosphatidylcholine membranes

CrossMark

Chee W. How [1], José A. Teruel, Antonio Ortiz, María F. Montenegro,
José N. Rodríguez-López, Francisco J. Aranda *

Departamento de Bioquímica y Biología Molecular-A, Universidad de Murcia, Campus de Espinardo, E-30100 Murcia, Spain

ABSTRACT

Catechin flavonoids are the main components of green tea extracts which present broad potential physiological activities. Several of their biological activities seem to affect membrane-dependent cellular processes and it is known that some catechins interact with phospholipid membranes. In this study we examine the interactions of a 3-O-(3,4,5-trimethoxybenzoyl)-($-$)-catechin (TMCG), and its quinone methide (QM) activated product with 1,2-dipalmitoyl-sn-glycero-3-phosphocholine (DPPC) membranes by means of differential scanning calorimetry, X-ray diffraction, Fourier-Transform infrared spectroscopy and molecular dynamics simulation. We report that there are extensive interactions between TMCG and DPPC involving the perturbation of the thermotropic gel to liquid crystalline phase transition of the phospholipid, the decrease of bilayer thickness and the promotion of interdigitated gel phase, together with an increase of the hydrogen bonding pattern of the interfacial region of the bilayer. In contrast, QM shows a weak interaction with the phospholipid bilayer. Molecular dynamics simulation indicates that TMCG locates in the interior of the bilayer, while QM is found interacting with the surface of the membrane. The observations are interpreted in terms of the mechanism of membrane prodrug activation and the underlying membrane perturbations of the biological actions of natural catechins.

© 2014 Elsevier B.V. All rights reserved.

1. Introduction

Catechin flavonoids are the main components of green tea extracts and a vast body of scientific evidence suggests that they are responsible for the majority of the potential health benefits attributed to green tea consumption. Catechins have received much attention due to their broad potential physiological activities. Some catechins have been found to have antibacterial, antifungal and/or antiviral activities [1–7] and several studies have demonstrated that catechins have antioxidant activity which may prevent oxidative damage in many organs [8–10].

However, an intense field of research has been focused on the anticancer properties of these polyphenol compounds [11–13]. In this regard, we early found that the ester-bonded gallate catechins, isolated from green tea, were potent inhibitors of dihydrofolate reductase (DHFR) at concentrations found in the serum and tissues of green tea drinkers [14,15]. Despite the excellent anticancer properties of tea catechins, they have one significant limitation: their poor bioavailability, which is related to their low stability in neutral or slightly alkaline solutions and their inability to cross cellular membranes easily [16]. In an attempt to solve such bioavailability problems, we synthesized a

3,4,5-trimethoybenzoyl analogue of epicatechin-3-gallate, TMECG, which showed high antiproliferative activity against malignant melanoma [17]. We observed that this compound effectively suppressed the proliferation of melanoma cells by inducing apoptosis [18] and that this drug can be used in combination with methotrexate as an effective and tissue-restricted antimelanoma therapy [19].

Because the major polyphenols present in tea have epicatechin configurations, many of the studies designed to elucidate the biological activities of these tea catechins have been performed with epicatechin derivatives, but catechin gallate also inhibits the proliferation of cancer cells derived from human oral cavity tissues [20]. As part of our on-going efforts to develop new tea-derived compounds, we synthesized a trimethoxybenzoyl analogue of catechin gallate (TMCG) [21]. A comparative study of the activity of both epimers in melanoma concluded that both were prodrugs that could be selectively activated by the specific melanocyte enzyme tyrosinase [21,22]. Upon activation, both TMECG and TMCG generated a stable quinone methide (QM) product that strongly inhibited DHFR in an irreversible manner [23]. We observed that oxidation of TMCG and TMECG by tyrosinase generated the same final product because proton-catalyzed hydrolysis of ring C would generate a freely rotating carbon (C-3), which should prevent epimeric differences in the QM active product (Fig. 1).

It is well established that the biological activity of green tea catechins affects membrane dependent cellular processes, such as cell signaling, cell cycle, arachidonic acid metabolism and mitochondrial functionality,
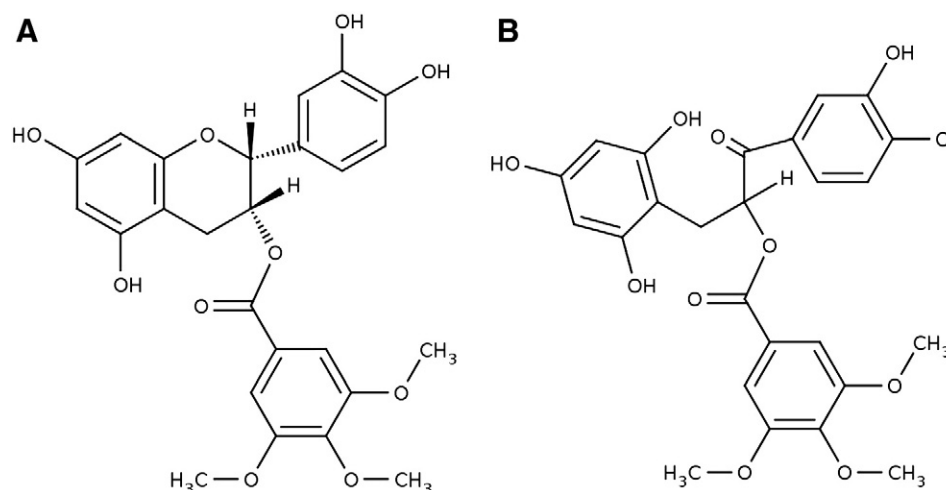
Fig. 1. Structure of 3-*O*-(3,4,5-trimethoxybenzoyl)-(−)-catechin (TMCG) (A) and its quinone methide activated product (QM) (B).

and it has been shown that they modulate numerous membrane proteins like proton ATPase [24], ion channels [25–27] and growth factor receptors [28]. Therefore, the interaction between catechins and membranes is currently an intense field of investigation.

It has been shown that catechins caused aggregation and leakage of contents from lipid vesicles [29–32] and that these compounds interact with the lipid bilayer [32–34]. In addition, it has been suggested that catechins may exert their effects on membrane function by a common bilayer mediated mechanism [27] and some authors have indicated that their interaction with the membrane correlates with their antioxidant and antibacterial effects [32,33]. Although human tyrosinase is an integral membrane protein and the amphiphilic nature of TMCG points to the membrane as its hypothetical site of action, nothing is known about the interaction between this antitumoral drug and membranes. In order to get insight into the mechanism of activation and transport of this drug and to explore other possible biological actions, it is important to know the influence of this drug on the lipid component of membranes. We have obtained this synthetic catechin derivative (TMCG) and its activated product (QM). We have used several techniques like differential scanning calorimetry (DSC), small and wide angle X-ray diffraction (SAXD and WAXD), Fourier-Transform infrared spectroscopy (FTIR) and molecular dynamics simulation (MD) to study the effect of these drugs on the thermotropic and structural properties of phosphatidylcholine, the most important phospholipid in eukaryotic membranes.

2. Materials and methods

2.1. Materials

1,2-Dipalmitoyl-*sn*-glycero-3-phosphocholine (DPPC) was obtained from Avanti Polar Lipids Inc. (Birmingham, AL). Phospholipid concentrations were determined by phosphorous analysis [35]. (−)-Catechin, 3,4,5-trimethoxybenzoyl chloride and mushroom tyrosinase were from Sigma Chemical Co. (Madrid, Spain). Purified water was deionized in a Milli-Q equipment from Millipore (Bedford, MA), and filtered through 0.24 μm filters prior to use. All other reagents were of the highest purity available. The synthesis of TMCG was carried out from the commercially available catechin, following a procedure previously described by our research group [21]. Mushroom tyrosinase was used to oxidize TMCG to its corresponding QM product [23].

2.2. Differential scanning calorimetry

The lipid mixtures for differential scanning calorimetry (DSC) measurements were prepared by combination of chloroform solutions containing DPPC and the appropriate amount of TMCG as indicated. The

organic solvents were evaporated under a stream of dry N_2, free of O_2, and the last traces of solvents were removed by further 3 h evaporation under high vacuum. To the dry samples, 2 ml of a buffer containing 150 mM NaCl, 0.1 mM EDTA, 10 mM Hepes pH 7.4 was added, and vesicles were formed by vortexing the mixture, always keeping the temperature above the gel to liquid-crystalline phase transition temperature of the phospholipid. In the case of QM containing samples, appropriate amounts of QM were added to the buffer before vesicle formation. Experiments were performed using a MicroCal MC2 calorimeter (MicroCal, Northampton, USA). The final phospholipid concentration was 1 mg ml^{-1}. The heating scan rate was 60°Ch^{-1}. The construction of partial phase diagrams was based on the heating thermograms for a given mixture of phospholipid and drug at various drug concentrations. The onset and completion temperatures for each transition peak were plotted as a function of the molar fraction of drug. These onset and completion temperatures points formed the basis for defining the boundary lines of the partial temperature-composition phase diagram.

2.3. X-Ray diffraction

Simultaneous small (SAXD) and wide (WAXD) angle X-ray diffraction measurements were carried out as described previously [36] using a modified Kratky compact camera (MBraum-Graz-Optical Systems, Graz Austria) which employs two coupled linear position sensitive detectors (PSD, MBraum, Garching, Germany). Nickel-filtered Cu K$_\alpha$ X-rays were generated by a Philips PW3830 X-ray Generator operating at 50 kV and 30 mA. Samples for X-ray diffraction were prepared by mixing 10 mg of phospholipids and the appropriate amount of TMCG in chloroform. Multilamellar vesicles were formed as described above, and when appropriate QM was added to the buffer before vesicle formation. After centrifugation at 13,000 rpm, the vesicles were placed in a steel holder, which provided good thermal contact to the Peltier heating unit, with cellophane windows. Typical exposure times were 10 min, allowing 10 min prior to the measurement for temperature equilibration. Background corrected SAXD data were analyzed using the program GAP (global analysis program) written by Georg Pabst and obtained from the author [37,38]. This program allowed to retrieve the membrane thickness, $dB = 2(zH + 2\sigma H)$ from a full q-range analysis of the SAXD patterns [39]. The parameters zH and σH are the position and width, respectively, of the Gaussian used to describe the electron-dense headgroup regions within the electron density model.

2.4. Infrared spectroscopy

For the infrared measurements, multilamellar vesicles were prepared in the same buffer prepared in D_2O as described above. Samples

were placed in between two CaF$_2$ windows (25 × 2 mm) separated by 25 μm Teflon spacers and transferred to a Symta cell mount. Infrared spectra were acquired in a Nicolet 6700 FTIR spectrometer (Madison, WI). Each spectrum was obtained by collecting 256 interferograms with a nominal resolution of 2 cm^{-1}. The equipment was continuously purged with dry air in order to minimize the contribution peaks of atmospheric water vapor. The sample holder was thermostatized using a Peltier device (Proteus system from Nicolet). Spectra were collected at 2 °C intervals, allowing 5 min equilibration between temperatures. The D$_2$O buffer spectra taken at the same temperatures were subtracted interactively using either Omnic or Grams (Galactic Industries, Salem, NH) software.

2.5. Molecular dynamics simulations

TMCG and QM molecules were constructed using PyMOL software [40]. To build the topologies of these structures, they were submitted to the PRODRG server [41], and the initial geometries of crude topologies were retrieved. Based on such information, these structures were described in GROMOS96 43a1 force field parameters [42]. Afterwards, both topologies were further modified to include some refinements. In order to calculate atomic charges both structures were submitted to full-geometry optimization using *ab initio* quantum-mechanical computations using Firefly QC package [43], which is partially based on the GAMESS (US) [44] source code, with a 6-31G basis set and restricted Harteree–Fock method. Hessian matrix analyses were employed to unequivocally characterize the optimized structures as true minima on the potential energy surface. These minimal energy conformations were submitted to single-point *ab initio* calculations to determine Löwdin atomic charges, and finally, these calculated atomic charges were used to construct their corresponding topology files. Bad charge grouping in the topology files may lead to incorrect results. Thus, for instance, small charge-groups may not be correctly chosen if the spatial extent is relatively large [45]. Therefore, to ensure that the spatial extent of our charge-groups was small, TMCG and QM molecules were parameterized by creating charge-groups containing no more than four contiguous atoms. DPPC topology file was obtained from Chiu et al. [46]. The systems studied comprised catechin derivatives, initially located in the water phase of a DPPC membrane. A monolayer was constructed with 36 DPPC molecules organized in a 6 rows and 6 columns arrangement to build up the DPPC bilayer. Then four TMCG or QM molecules were randomly located over the lipid monolayer and then transposing another layer to form the bilayer structure with the catechin molecules out of the lipid membrane, yielding a 9:1 DPPC/catechin ratio. A total of 3750 water molecules (52 waters/lipid) were added to the lipid bilayer containing the catechin derivatives to create a fully hydrated system, with the drugs located in the water phase. In the case of QM sodium ions were also added as counterions in the water phase, to assure electrical neutrality of the system. For water the generic single point charge (SPC) water configuration [47] was used. The lipid bilayer was aligned such that it lied in the XY plane, i.e., the monolayers normal was parallel to the Z-axis. Molecular dynamics calculations were carried out with GROMACS v4.5 molecular simulation package [48] under constant number of particles, pressure and temperature. Gromacs 43A1-S3 force field, which is an improved force field for lipids based on GROMOS96 43a1, was used [46]. All simulations were performed in the NPT ensemble. Pressure control was carried out using the weak-coupling Berendsen scheme with coupling time of 1.0 ps and semi-isotropic pressure coupling (isotropic in the x and y direction, but different in the z direction). Periodic boundary conditions were applied in all directions. Temperature control was carried out with a V-rescale thermostat with coupling time of 0.1 ps [49]. All bonds were constraint using the SETTLE algorithm [50] for water and the LINCS algorithm for all other bonds [51]. A leap-frog integration scheme with a time-step of 2 fs was used. The Particle Mesh Ewald method was used to correct for long-range electrostatic interactions [52], and short-range electrostatic and van der Waals interactions were cut off at 1.2 nm [53,54]. Molecular dynamic simulations were carried out for mixtures of DPPC + TMCG and DPPC + QM bilayers at a constant pressure of 1 bar and 323 K, above the main phase transition temperature of DPPC. In all cases molecular dynamics simulations were preceded by energy minimization using the steepest descent algorithm [55] to remove any steric clashes or inappropriate geometries. At least 300 ns molecular dynamic simulations were carried out to allow relaxation and equilibration of the systems, followed by a second 100 ns run. Finally, the last 50 ns were collected for all calculations. Viewers VMD 1.8.2 [56] and PyMOL 1.5.0.1 [40] were employed to roughly inspect the arrangement of the catechin derivatives molecules in the lipid matrix and water phase and to capture images throughout the corresponding trajectories.

3. Results and discussion

3.1. Differential scanning calorimetry

The molecular interaction of TMCG and QM with membranes has been investigated using lipid vesicles formed by DPPC. DSC was used to characterize the influence of these drugs on the thermotropic properties of DPPC, and their effect on the macroscopic organization and structural properties of the phospholipid was studied by means of X-ray diffraction and infrared spectroscopy.

The influence of TMCG on the thermotropic gel to liquid crystalline phase transition of DPPC is depicted in Fig. 2A. In the absence of the drug, pure DPPC (top thermogram) exhibits two endotherms upon heating: a lower temperature lower enthalpy pretransition at 35 °C which separate the Lβ' gel phase from the Pβ' rippled gel phase, and a higher temperature higher enthalpy main transition at 41 °C from the rippled gel phase to the Lα liquid crystalline phase respectively, in agreement with previous results [57,58]. The thermotropic pretransition of DPPC is greatly affected by the presence of a very low concentration of TMCG, being already abolished at a TMCG mol fraction of 0.02. Increasing concentrations of TMCG progressively broaden the main transition and cause a shift to lower temperatures. The presence of TMCG at concentration higher than 0.10 molar fraction produces the appearance of several broad endotherms, the lower temperature peak with a midpoint transition temperature of 27.7 °C increases in size as more TMCG is present in the membrane so that in the presence of the highest concentration
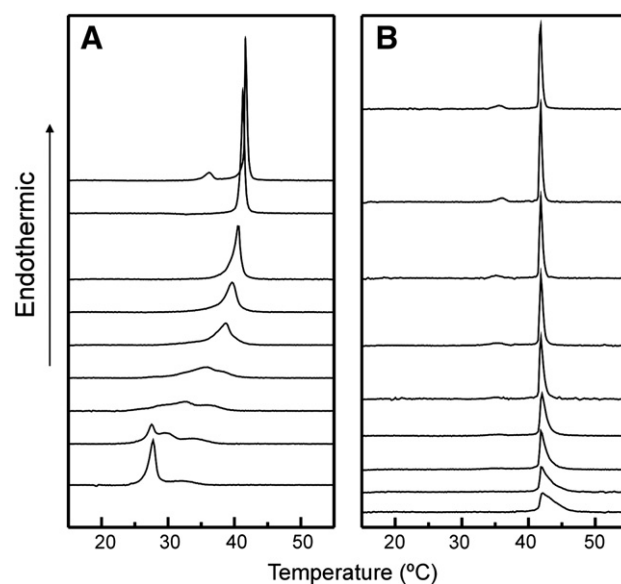

Fig. 2. DSC heating thermograms for DPPC containing TMCG (A) or QM (B) at different concentrations. Molar fraction of catechin derivatives from top to bottom: 0, 0.02, 0.05, 0.07, 0.10, 0.15, 0.20 and 0.30.

(0.30 molar fraction) this peak which shows high cooperativity is the predominant one. These effects could be explained by the establishment of a molecular interaction between the phospholipid acyl chains and the TMCG molecule. This interaction would be the consequence of the intercalation of the TMCG molecule between the phospholipids. The alignment of part of TMCG with the phospholipids acyl chains can disrupt the phospholipid packing, reduce the cooperativity of the transition and shift the phase transition temperature to lower values. However, all phospholipid molecules undergo the transition as the total enthalpy change of the transition (i.e. the area under the peaks) did not significantly change (data not shown). The appearance of several melting component in the thermograms when the concentration of TMCG is increased can be explained by the formation of TMCG enriched domains, but the apparition of the predominantly cooperative peak with midpoint transition temperature at 27.7 °C suggests the formation of a stable complex or a different phase as will be discussed below. The effect of QM on the DPPC thermotropic transition (Fig. 2B) is completely different to that described above for TMCG. A broad pretransition is still observed even at a QM molar fraction of 0.15. This lack of effect on the pretransition, which is very sensitive to the presence of foreign molecules into the bilayer, and the fact that the main onset transition temperature does not change even at the highest concentration used suggests that QM does not incorporate very efficiently into the phospholipid palisade. The enthalpy change of the transition did not change significantly (data not shown). However, the shift of the end of the main transition to higher temperatures suggests that the gel phase is more stable as more QM is present in the membrane pointing out to a surface interaction between the QM and DPPC.

3.2. X-Ray diffraction

Information on the structural characteristics of DPPC/TMCG systems was obtained by SAXD. Phospholipids, when organized into multilamellar structures, should give rise to reflections with relative distances of 1:1/2:1/3… [59]. Fig. 3 shows the small angle X-ray diffraction pattern profiles corresponding to pure DPPC and DPPC containing TMCG at different temperatures. Pure DPPC produces several reflections with relative distances of 1:1/2:1/3, which is consistent with their expected multilamellar organization. This technique not only defines the macroscopic structure itself, but also provides the interlamellar repeat distance in the lamellar phase. The largest first order reflection component corresponds to the interlamellar repeat distance (d-value), which is comprised of the bilayer thickness and the thickness of the water

layer between bilayers. DPPC gives rise to a first order reflection with a d-value of 62.5 Å in the Lβ' gel state (20 °C), 72.5 Å in the Pβ' rippled phase (38 °C) and 64.1 Å in the Lα liquid crystalline state (45 °C) (Fig. 3), in agreement with previous data [60,61]. Samples containing TMCG give rise to two or three reflections which related as 1:1/2:1/3 in the whole range of temperatures under study, confirming that the presence of TMCG does not alter the lamellar structural organization of the phospholipids. However, TMCG did affect the interlamellar repeat distance depending on concentration. At 20 °C, the system containing TMCG at 0.07 molar fraction shows a d-value of 72 Å which is similar to that found in the pure phospholipid in the rippled phase. At 20 °C and 38 °C, the system containing TMCG at 0.15 molar fraction shows d-values of 69.3 Å and 68.1 Å which are intermediate between those of the rippled phase and the liquid crystalline phase. The effect of TMCG at 0.30 molar fraction is drastic because a very short d-value of 45.7 Å is found at 20 °C. This repeating distance is characteristic of the interdigitated gel phase in which the hydrocarbon chains of the two lipid layers are fused, making it possible to form tighter packing. At higher temperatures a value of 60.1 Å is found for this system. An apparent membrane thinning effect of some catechins has been described before [31,32].

We carried out experiments in the wide angle region (WAXD) reporting on the chain lattice in order to obtain information about the packing of the DPPC acyl chains in the presence of TMCG. Fig. 4 shows the WAXD pattern corresponding to pure DPPC and DMPC containing TMCG at different temperatures. As shown in Fig. 4, pure DPPC at 20 °C, i.e. below the pretransition, gives a sharp reflection centered at 4.19 Å and a broad one at 4.10 Å. This type of pattern is typical of an Lβ' phase and corresponds to a quasihexagonal lattice in which the acyl chains are tilted with respect to the bilayer normal forming one group of four closely spaced chains with two chains at a slightly larger separation [62]. At 38 °C, i.e. above the pretransition, a single reflection appears around 4.15 Å. which is attributed to a lipid phase with hydrocarbon chains being oriented normal to the bilayer plane in a two-dimensional hexagonal lattice as described for the Pβ' phase [63] in accordance with the data described above with SAXD. This reflection is, however, considerably broader than the corresponding peak of conventional Lβ phases formed in other phospholipid system like phosphatidylethanolamine [64] reflecting the tilt of the chains in the Pβ' phase. At 45 °C, the pattern for the Lα phase, as would be expected, consists of a single broad diffuse reflection. At 20 °C in the presence of TMCG at 0.07 and 0.15 molar fraction the system shows the
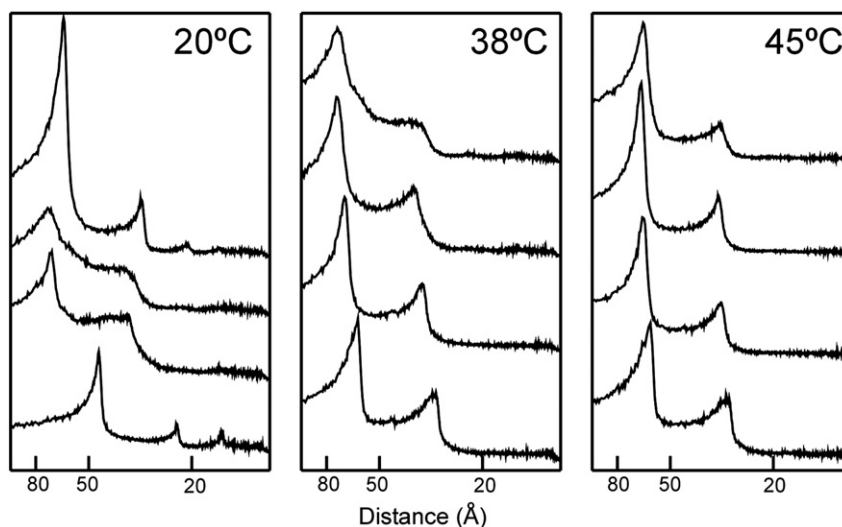

Fig. 3. Small angle X-ray diffraction (SAXD) profiles of DPPC system containing different concentration of TMCG at different temperatures. From top to bottom: pure DPPC, DMPG containing 0.07 mol fraction TMCG, DPPC containing 0.15 mol fraction TMCG and DPPC containing 0.30 mol fraction TMCG.
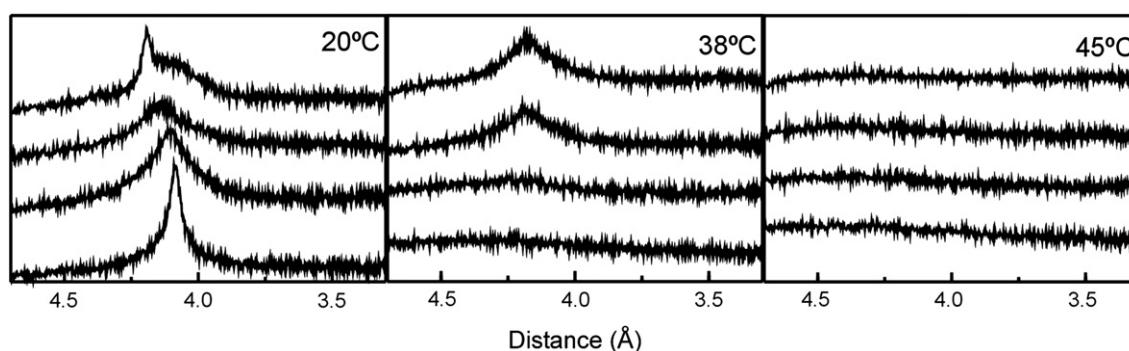
Fig. 4. Wide angle X-ray diffraction (WAXD) profiles of DPPC system containing different concentration of TMCG at different temperatures. From top to bottom: pure DPPC, DMPG containing 0.07 mol fraction TMCG, DPPC containing 0.15 mol fraction TMCG and DPPC containing 0.30 mol fraction TMCG.

characteristic pattern of the rippled phase, indicating that the disappearing of the pretransition observed by DSC is due to a lowering of the pretransition temperature and broadening of the peak. At 38 °C the system containing 0.07 molar fraction of TMCG is still in the rippled phase, however in the presence of 0.15 molar fraction of TMCG this reflection is very broad suggesting that part of the lipid has already undergone the transition to the L_α phase, which is consistent with the decrease of the phase transition temperature found in the DSC experiments. At 45 °C, the presence of TMCG at 0.07 and 0.15 molar fraction does not affect the packing of the DMPC acyl chains in the liquid-crystalline phase. In the presence of 0.3 molar fraction of TMCG, the wide angle scattering peaks recorded at 20 °C all reside at a spacing of 4.1 Å and the symmetric feature and sharpness of the intensity profile indicates that the lipids are in the nontilted gel interdigitated phase in accordance with the SAXD data, at higher temperatures the characteristic single broad diffuse reflection of the liquid crystalline phase is found.

Background-subtracted SAXD patterns for DPPC and DPPC/TMCG at 0.30 molar fraction were analyzed using the global analysis program (GAP) to confirm the formation of an interdigitated phase in the presence of high concentration of TMCG. Fig. 5 shows the corresponding one-dimensional electron density profiles along the bilayer normal calculated from the SAXD diffraction patterns. The profile for pure DPPC contains a central region of relatively low electron density values corresponding to the hydrocarbon chains of the phospholipid molecules; a region of relatively high electron density corresponding to the headgroups, which symmetrically border the hydrocarbon region; and an interstitial solvent-rich layer with electron density values intermediate between those of the first two regions. The bilayer is centered at the origin, so that the low electron density trough at 0 Å corresponds to the terminal methyl groups in the bilayer center. For pure DPPC below the main transition temperature (Fig. 5) we found a bilayer thickness of 52.3 Å and a water layer distance of 9.4 Å. The presence of TMCG altered three structural features. First, the bilayer thickness distance decreased to 41.3 Å, indicating that the bilayers became thinner in the presence of this concentration of TMCG. Second, the terminal methyl trough disappeared as the electron density in the bilayer center became more uniform. Third, the width of the water layer between opposing bilayers also decreased to 3.9 Å. The shape of this profile is similar to that previously observed for interdigitated phase bilayers [65–67] confirming the presence of this phase in this system. Above the phase transition temperature both systems organize in a liquid crystalline phase, although in the presence of TMCG the bilayer thickness is still a bit thinner (42.7 Å compared with 46.6 Å for the pure phospholipid). The existence of interdigitated membranes in the presence of TMCG, though present at high TMCG concentration in the gel ordered state might be relevant for some action mediated by catechins as it has been speculated that catechins may accumulate in tissues over time to produce cellular concentrations that are much higher than those observed in clinical serum samples [68] and it has been proposed that catechins interact with

ordered lipid raft domains in membranes [69]. In addition it is important to note that the modulation of bilayer thickness may regulate membrane protein function [70].

Fig. 6 shows the small and wide X ray diffraction pattern for DPPC containing 0.25 molar fraction of QM. At 20 °C the mixture shows a d-value of 61.5 Å (Fig. 6A), very close to that found for the pure phospholipid, and the peak and shoulder in the WAXD pattern (Fig. 6B) indicate that the system is in the Lβ′ phase. At 38 °C the first order SAXD reflection give a d-value of 66.9 Å, which is larger than that of the regular nonrippled gel phase, the asymmetric WAXD reflection suggests that a nonrippled phase is present at this temperature. At 50 °C the SAXD and WAXD pattern indicate that the system is in the liquid crystalline phase, however, the d-value of 67.5 Å obtained at this temperature is larger than that of the pure phospholipid (64.1 Å). Background-subtraction of the SAXD pattern and analysis using the global analysis program (GAP) indicates that this increase in d-value is due to an
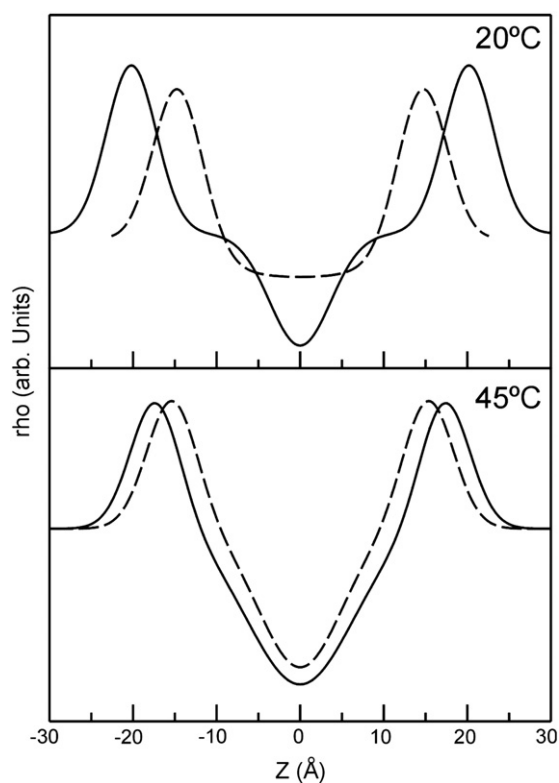

Fig. 5. One-dimensional electron density profiles calculated from SAXD profiles of pure DPPC (solid line) and DPPC containing TMCG at 0.30 molar fraction (dashed line) at different temperatures, using the GAP program.
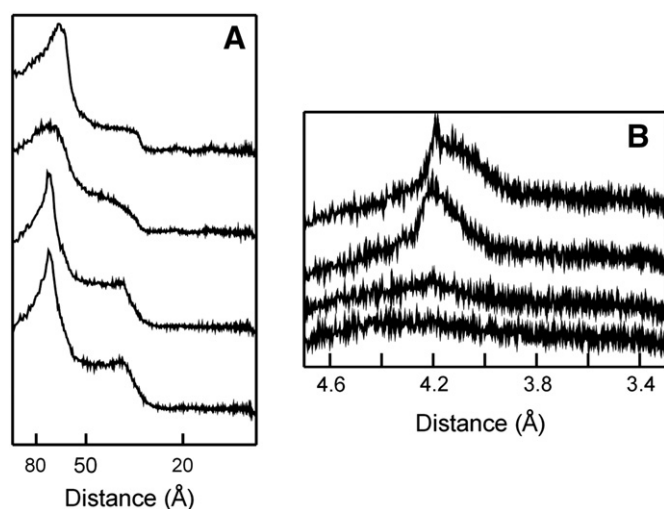
Fig. 6. Small angle X-ray diffraction (SAXD) (A) and wide angle X-ray diffraction (WAXD) (B) profiles of DPPC system containing 0.25 molar fraction QM, at different temperatures. From top to bottom: 20 °C, 38 °C, 45 °C and 50 °C.

effective increase in the width of the water layer between bilayers (data not shown).

Partial phase diagrams for the DPPC component in mixtures of the phospholipid and catechin derivatives were constructed using the DSC data and the information of phospholipid structural organization obtained from SAXD/WAXD. The onset and the completion temperatures of the heating thermograms shown in Fig. 2 gave the points to obtain the solid and fluid lines of the phase diagrams, respectively. In the case of the DPPC/TMCG system (Fig. 7 left) both the solid (up to a 0.15 molar fraction of TMCG) and the fluid (in the whole range of concentration) lines display a near ideal behavior, the temperature decreasing as the TMCG concentration increases. The system evolves from a lamellar gel phase (G phase) to a lamellar liquid-crystalline phase (F phase) through a coexistence region (G + F) which is wider as more TMCG is present in the system. However at molar fractions higher than 0.15, the solid line behaves differently remaining nearly horizontal, indicating the existence of a gel phase immiscibility and evidencing the formation of the interdigitaded gel phase, immiscible in the gel phase. The system evolves from an interdigitated gel phase (I phase) to a liquid crystalline phase (F phase) through a complex coexistence region (I + G + F). In the presence of QM (Fig. 7 right), the solid line keeps horizontal in the whole range of QM, indicating the presence of an immiscibility in the gel phase between pure DPPC and a population of phospholipids which interact with the QM. The fluidus line shows a moderate increase in temperature reflecting the stabilization

of the gel phase produced in the population of phospholipids interacting with QM. The system evolves from an immiscible gel phase in which different gel phases coexist (G′ phase) to a liquid crystalline phase (F phase) through a coexistence region (G′ + F).

3.3. Infrared spectroscopy

We used infrared spectroscopy to study the interfacial interaction between catechin derivatives and the membrane. The C＝O stretching region of the phospholipid infrared spectra includes information about lipid interfacial hydration-hydrogen bonding interaction, and thus gives details of the intermolecular interaction that occurs in this domain. The C＝O stretching band of diacylphosphatidylcholines is a fairly broad band around 1750–1700 cm^{-1}, and seems to be a summation of subcomponents centered near 1741 and 1727 cm^{-1} [71]. The relative intensities of these component bands reflect the contribution of sub-populations of dehydrated and hydrated carbonyl groups [72]. Fig. 8 shows the temperature dependence of the frequency at the absorbance maximum of the C＝O stretching band of the infrared spectra of pure DPPC and mixtures with TMCG and QM. Pure DPPC shows absorption maxima at 1733 cm^{-1} and 1730 cm^{-1} in the gel and liquid-crystalline state respectively, according to previous data [58], the gel to liquid-crystalline phase transition producing a shift of the maximum frequency to lower values, reflecting the increase in intensity of the underlying component band at 1727 cm^{-1}, attributed to a higher amount of hydrogen bonded carbonyl groups resulting from a phase state-induced increase in the hydration of the polar–apolar interface [71]. The broadening and shift of the phase transition to lower temperatures produced by the presence of TMCG can be also observed following the maximum of the C＝O band depicted in Fig. 8. It is interesting to note than the presence of TMCG produces a shift of the maximum of the C＝O band to lower frequencies as compared to pure phospholipid, both in the gel and liquid-crystalline phase. This decrease in frequency indicates an increase in the proportion of hydrogen bonded C＝O component at all temperatures and suggests that TMCG interacts with the interfacial region of the DPPC bilayer, increasing the hydrogen bonding of the C＝O groups probably with the hydroxyl groups of the catechin derivative. An increase in the degree of hydration of the phosphate group of a different phosphatidylcholine has been described previously for some catechins [33]. The observed interdigitation can be understood if we consider the location of the TMCG molecules in the bilayer. The hydroxyl groups of the TMCG molecules bind to the carbonyl group of the lipid headgroup and the rest of the TMCG molecule is located into the hydrophobic core of the bilayer. Since the OH-group binds to the carbonyl moiety of the lipid headgroup lateral space would be created between the headgroups, leading to voids in the hydrophobic core that would destabilize the gel phase. These voids are energetically unfavorable and it
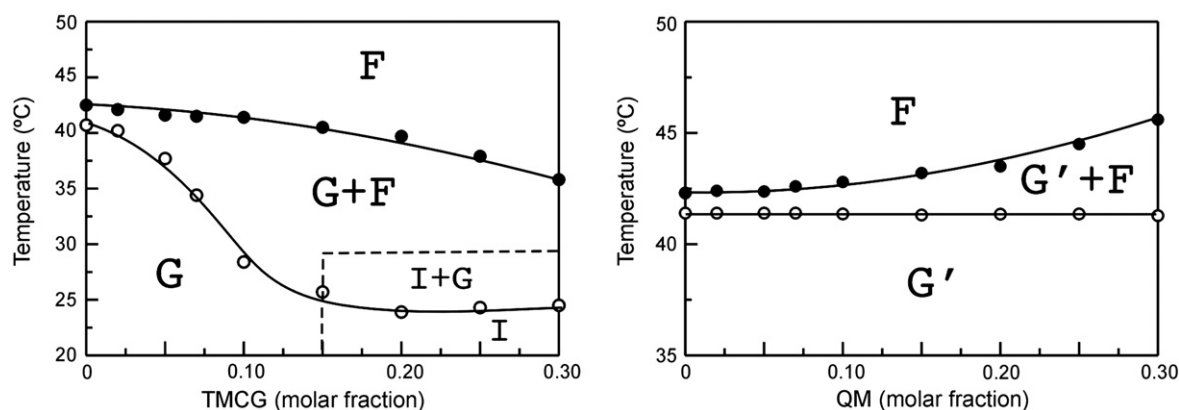

Fig. 7. Partial phase diagrams for DPPC in DPPC/TMCG (left) and DPPC/QM (right) mixtures. Open and solid circles were obtained from the onset and completion temperatures of the main gel to liquid crystalline phase transition. The phase designations are as follows: G, gel phase; F, liquid crystalline phase; I, interdigitated gel phase and G′, immiscible gel phases.
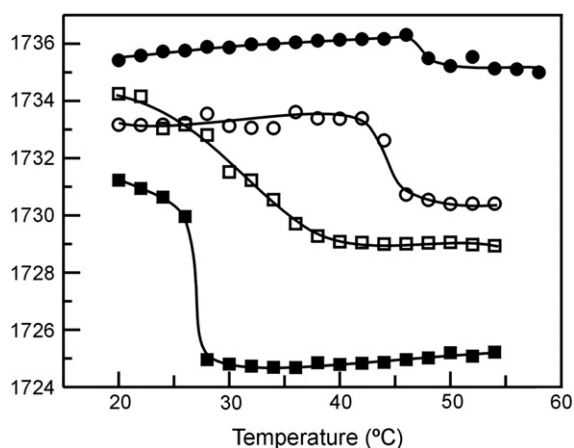
Fig. 8. Temperature dependence of the maximum of the carbonyl stretching absorption band exhibited by pure DPPC (○), DPPC/TMCG mixtures at 0.15 (□) and 0.30 (■) molar fraction, and DPPC/QM mixture at 0.25 (●) molar fraction.

has been shown that bilayer systems will minimize that energy by the formation of an interdigitated phase [73]. Since the tail ends of the TMCG molecules shield the tail ends of the lipids from the interfacial water, the energy cost in the formation of the interdigitated phase is minimized. In the presence of QM it can be seen that the transition temperature is moderately shifted towards higher temperatures in accordance with the thermotropic behavior described above for the system in the presence of high concentration of this quinone. It is intriguing to note that at difference with the behavior described for TMCG, the presence of high concentration of QM produces a shift of the maximum of the C=O band to higher frequencies, both in the gel and liquid-crystalline phase. This increase in frequency indicates an increase in the proportion of dehydrated C=O component at all temperatures and suggests that QM interacts with the interfacial region of the DPPC bilayer, decreasing the hydrogen bonding of the C=O groups with the water molecules of the hydration layer. The hydroxyl groups of QM will participate in hydrogen bonds with water, leaving less water molecules available to interact with the phospholipids. This dehydration of the interfacial region has been shown to correlate with a decrease of lipid mobility [74] and thus may explain the stabilization of the gel phase, i.e. higher end transition temperature observed by DSC.

3.4. Molecular dynamics simulations

Molecular dynamics simulations have been performed to study the location of both TMCG and QM in the DPPC bilayer. Our analysis starts with the density profiles of all components along the z-axis which is normal to the two DPPC leaflets. Both catechin derivatives were placed initially in the water phase and in the course of the simulation, they interact with the bilayer. The exact distribution of all components is given in Fig. 9A and B, in which it is clear how the TMCG molecule prefers being in the interior of the DPPC bilayer with part of the molecule near the water interface, and how the QM molecule has predominantly interfacial interactions adsorbed onto the surface. To get a general view of how TMCG and QM are distributed in the membrane, selected snapshots of the TMCG/DPPC and QM/DPPC systems are shown in Fig. 9C and D as representative pictures. It is important to note that the methoxy groups are the part of the TMCG molecule which locate deepest into the bilayer (data not shown), emphasizing the importance of this chemical modification for the interaction of the drug with the membrane.

Molecular dynamics calculations shows that TMCG prefers to locate in the interior of DPPC bilayers and in this way it may perturb the phospholipid palisade and affect the thermotropic phase transition of the phospholipid, altering the thickness of the membrane and increasing

the hydrogen bonding pattern of the interfacial region. At difference with the later, molecular dynamics shows a surface interaction for QM which agrees with its weak effect on the phospholipid phase transition and structural parameter of the bilayer. Theses finding might be fundamental to understand the mechanism for the activation or TMCG and TMECG prodrugs in melanoma [22], in this sense both TMCG and TMECG will have a strong affinity for the bilayer membrane, which is important given the membrane location of human tyrosinase. Although these catechins are good substrates of this enzyme, once they have been activated to their corresponding QM, the soluble nature of this compound makes it to leave the membrane and enter into the soluble phase, where it can efficiently bind and inhibit DHFR its molecular target. In addition, the findings presented in this paper, in relation to the interaction between TMCG and phospholipid membranes, will contribute to understand the role of natural chatechins as bioactive agents and open the possibility of the potential use of this synthetic derivative in other health-promoting action of natural catechins.

4. Conclusions

The aim of this work was to characterize the interactions of an antitumoral synthetic catechin derivative TMCG and its activated QM product with phosphatidylcholine membranes. Our DSC data supported that TMCG is able to incorporate into DPPC membranes and to intercalate between the phospholipids molecules, where it can reduce the cooperativity and lower the transition temperature of the gel to liquid-crystalline phase transition. TMCG is able to form enriched domains and at higher concentration a new gel phase is found. X-Ray diffraction measurements indicated that TMCG did not affect the macroscopic bilayer organization of DPPC, but the presence of TMCG produced a decrease of the bilayer thickness with the formation of an interdigitated gel phase. Infrared experiments revealed that the TMCG increased the hydrogen bonding of the carbonyl interfacial group of the phospholipid. On the other hand, QM showed limited interaction with the phospholipid bilayer indicating a superficial interaction with a weak gel stabilizing effect and producing a decreased of the hydrogen bonding pattern of the interfacial region of the phospholipid. Our molecular dynamics simulation studies showed that TMCG is incorporated into the phospholipid palisade while QM is excluded from the bilayer and interact weakly with the polar part of the bilayer. Taken together, all these results point out to TMCG as a membrane interacting compound which could easily reach tyrosinase at its membrane location and form its activated QM product, which will leave the membrane and reach its soluble enzyme target. In view of the important health beneficial effects of natural catechins the results presented in this paper would also contribute to understand the molecular mechanism underlying their membrane related biological actions.

On the other hand, this study could be of interest for the design of novel antimelanoma drugs. Melanoma, a highly aggressive skin cancer, is resistant to many conventional therapies. Accumulating evidence has indicated that melanosomes contribute to the refractory properties of melanoma cells by sequestering cytotoxic drugs and increasing melanosome-mediated drug export [75–78]. Thus, lipophilic drugs or those transported by specific receptor can be trapped into the cellular endosomal–melanosomal system, being then, exported out of melanoma cells. Based on these observations, it has been suggested that preventing melanosomal sequestration of cytotoxic drugs may have great potential as an approach to improving the chemosensitivity of melanomas [79]. The results, obtained in this report, point out to the possibility of the use of catechin as an effective drug carrier. Esterification of catechin with pre-existing drugs could represent a strategy to prevent their melanoma export; thus, after tyrosinase-mediated oxidation of the catechin unit, the corresponding QM could be liberated from the cellular endosomal–melanosomal system and released in other cellular compartments to carry out their cytotoxic action.
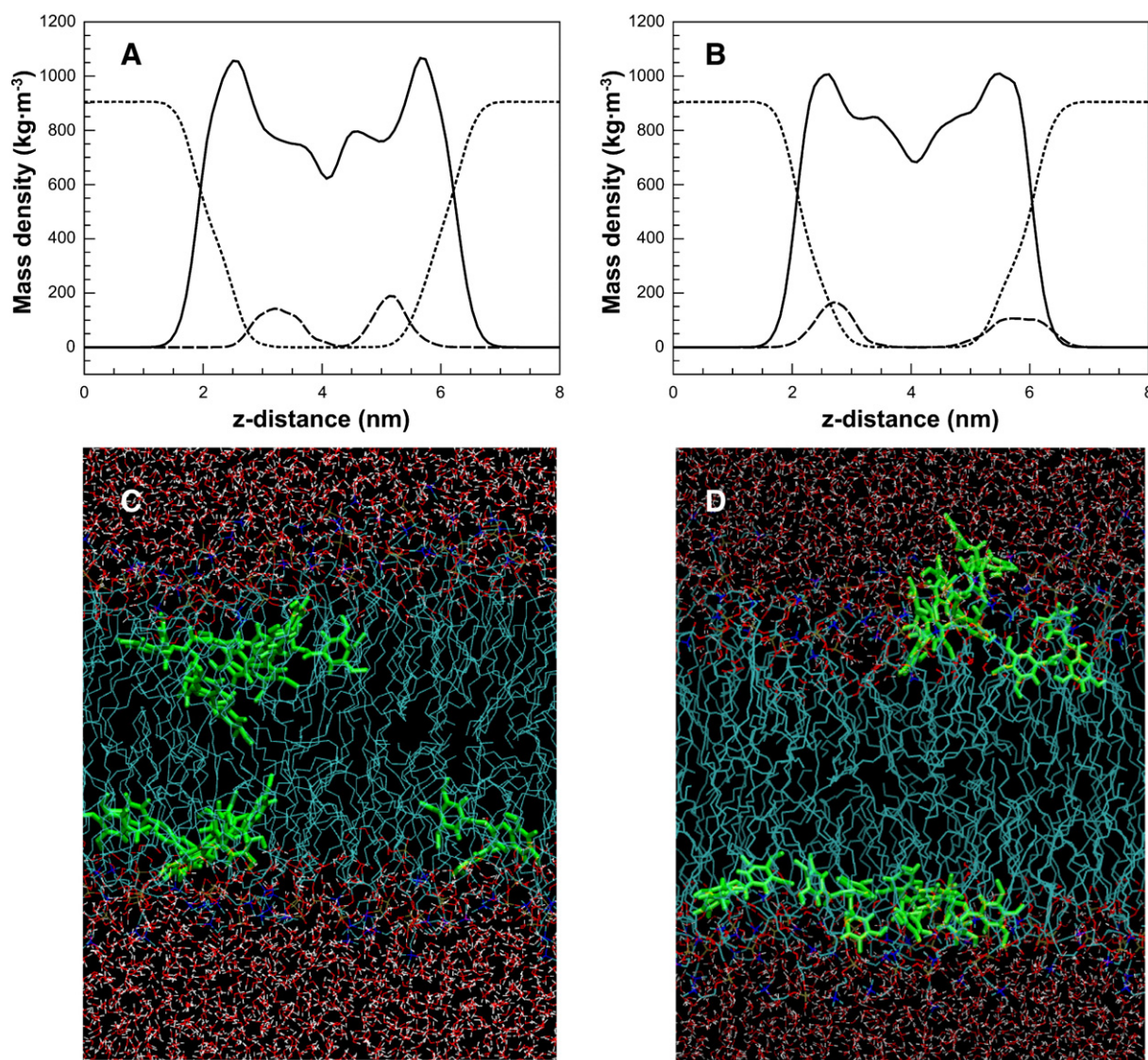
Fig. 9. Molecular dynamics simulation on the interaction of TMCG and QM with DPPC bilayers. Mass density profiles of water (dotted), DPPC bilayers (solid) and TMCG (A, dashed) or QM (B, dashed) are presented. Snapshots of the DPPC bilayers with TMCG (C) or QM (D). The system is periodic in all directions, and as such, the aqueous phase is continuous and catechin derivatives can interact with both bilayer surfaces. Red dots correspond to water molecules, blue lines to DPPC molecules, and light-green lines to TMCG (C) and QM (D) molecules.

References

[1] K. Mabe, M. Yamada, I. Oguni, T. Takahashi, In vitro and in vivo activities of tea catechins against *Helicobacter pylori*, Antimicrob. Agents Chemother. 43 (1999) 1788–1791.

[2] Y. Cui, Y.J. Oh, J. Lim, M. Youn, I. Lee, H.K. Pak, W. Park, W. Jo, S. Park, AFM study of the differential inhibitory effects of the green tea polyphenol (−)-epigallocatechin-3-gallate (EGCG) against gram-positive and gram-negative bacteria, Food Microbiol. 29 (2012) 80–87.

[3] J. Steinmann, J. Buer, T. Pietschmann, E. Steinmann, Anti-infective properties of epigallocatechin-3-gallate (EGCG), a component of green tea, Br. J. Pharmacol. 168 (2013) 1059–1073.

[4] B.J. Park, J.C. Park, H. Taguchi, K. Fukushima, S.H. Hyon, K. Takatori, Antifungal susceptibility of epigallocatechin 3-O-gallate (EGCg) on clinical isolates of pathogenic yeasts, Biochem. Biophys. Res. Commun. 347 (2006) 401–405.

[5] Y. Han, Synergic anticandidal effect of epigallocatechin-O-gallate combined with amphotericin B in a murine model of disseminated candidiasis and its anticandidal mechanism, Biol. Pharm. Bull. 30 (2007) 1693–1696.

[6] J.M. Song, H. Lee, B.L. Seong, Antiviral effect of catechins in green tea on influenza virus, Antiviral Res. 68 (2005) 66–74.

[7] S. Li, T. Hattori, E.N. Kodama, Epigallocatechin gallate inhibits the HIV reverse transcription step, Antivir. Chem. Chemother. 21 (2011) 239–243.

[8] T. Yokozawa, E.J. Cho, Y. Hara, K. Kitani, Antioxidative activity of green tea treated with radical inhibitor 2,29-azobis(2-amidinopropane) dihydrochloride, J. Agric. Food Chem. 48 (2000) 5068–5073.

[9] X. Shi, J. Ye, S.S. Leonard, M. Ding, V. Vallyathan, V. Castranova, Y. Rojanasakul, Z. Dong, Antioxidant properties of (−)-epicatechin-3-gallate and its inhibition of Cr (VI)-induced DNA damage and Cr (IV)- or TPA-stimulated NF-Kappa B activation, Mol. Cell. Biochem. 206 (2000) 125–132.

[10] A. Pękal, P. Dróżdż, M. Biesaga, K. Pyrzynska, Screening of the antioxidant properties and polyphenol composition of aromatised green tea infusions, J. Sci. Food Agric. 92 (2012) 2244–2249.

[11] C.S. Yang, J.D. Lambert, J. Ju, G. Lu, S. Sang, Tea and cancer prevention: molecular mechanisms and human relevance, Toxicol. Appl. Pharmacol. 224 (2007) 265–273.

[12] H. Fujiki, K. Imai, K. Nakachi, M. Shimizu, H. Moriwaki, M. Suganuma, Challenging the effectiveness of green tea in primary and tertiary cancer prevention, J. Cancer Res. Clin. Oncol. 138 (2012) 1259–1270.

[13] G.J. Du, Z. Zhang, X.D. Wen, C. Yu, T. Calway, C.S. Yuan, C.Z. Wang, Epigallocatechin Gallate (EGCG) is the most effective cancer chemopreventive polyphenol in green tea, Nutrients 4 (2012) 1679–1691.

[14] E. Navarro-Peran, J. Cabezas-Herrera, F. Garcia-Canovas, M.C. Durrant, R.N. Thorneley, J.N. Rodríguez-López, The antifolate activity of tea catechins, Cancer Res. 65 (2005) 2059–2064.

[15] E. Navarro-Peran, J. Cabezas-Herrera, L. Sánchez-del-Campo, J.N. Rodríguez-López, Effects of folate cycle disruption by the green tea polyphenol epigallocatechin-3-gallate, Int. J. Biochem. Cell Biol. 39 (2007) 2215–2225.

[16] J. Hong, H. Lu, X. Meng, J.H. Ryu, Y. Hara, C.S. Yang, Stability, cellular uptake, biotransformation, and efflux of tea polyphenol (−)-epigallocatechin-3-gallate in HT-29 human colon adenocarcinoma cells, Cancer Res. 62 (2002) 7241–7246.

[17] L. Sánchez-del-Campo, F. Otón, A. Tárraga, J. Cabezas-Herrera, S. Chazarra, J.N. Rodríguez-López, Synthesis and biological activity of a 3,4,5-trimethoxybenzoyl ester analogue of epicatechin-3-gallate, J. Med. Chem. 51 (2008) 2018–2026.

[18] L. Sánchez-del-Campo, J.N. Rodríguez-López, Targeting the methionine cycle for melanoma therapy with 3-O-(3,4,5-trimethoxybenzoyl)-(−)-epicatechin, Int. J. Cancer 123 (2008) 2446–2455.

[19] M. Sáez-Ayala, M.F. Montenegro, L. Sánchez-Del-Campo, M.P. Fernández-Pérez, S. Chazarra, R. Freter, M. Middleton, A. Piñero-Madrona, J. Cabezas-Herrera, C.R. Goding, J.N. Rodríguez-López, Directed phenotype switching as an effective antimelanoma strategy, Cancer Cell 24 (2013) 105–119.

[20] H. Babich, H.L. Zuckerbraun, S.M. Weinerman, In vitro cytotoxicity of (−)-catechingallate, a minor polyphenol in green tea, Toxicol. Lett. 171 (2007) 171–180.

[21] M. Sáez-Ayala, L. Sánchez-del-Campo, M.F. Montenegro, S. Chazarra, A. Tárraga, J. Cabezas-Herrera, J.N. Rodríguez-López, Comparison of a pair of synthetic tea-catechin-derived epimers: synthesis, antifolate activity, and tyrosinase-mediated activation in melanoma, Chem. Med. Chem. 6 (2011) 440–449.

[22] L. Sánchez-del-Campo, A. Tárraga, M.F. Montenegro, J. Cabezas-Herrera, J.N. Rodríguez-López, Melanoma activation of 3-o-(3,4,5-trimethoxybenzoyl)-(−)-epicatechin to a potent irreversible inhibitor of dihydrofolate reductase, Mol. Pharm. 6 (2009) 883–894.

[23] L. Sánchez-del-Campo, S. Chazarra, M.F. Montenegro, J. Cabezas-Herrera, J.N. Rodríguez-López, Mechanism of dihydrofolate reductase downregulation in melanoma by 3-O-(3,4,5-trimethoxybenzoyl)-(−)-epicatechin, J. Cell. Biochem. 110 (2010) 1399–1409.

[24] J. Zheng, V.D. Ramirez, Inhibition of mitochondrial proton F0F1-ATPase/ATP synthase by polyphenolic phytochemicals, Br. J. Pharmacol. 130 (2000) 1115–1123.

[25] B.H. Choi, J.S. Choi, D.S. Min, S.H. Yoon, D.J. Rhie, Y.H. Jo, M.S. Kim, S.J. Hahn, Effects of (−)-epigallocatechin-3-gallate, the main component of green tea, on the cloned rat brain Kv1.5 potassium channels, Biochem. Pharmacol. 62 (2001) 527–535.

[26] K. Kelemena, C. Kieseckera, E. Zitrona, A. Bauera, E. Scholza, R. Bloehsa, D. Thomasa, J. Gretena, A. Remppisa, W. Schoelsb, H.A. Katusa, C.A. Karlea, Green tea flavonoid epigallocatechin-3-gallate (EGCG) inhibits cardiac hERG potassium channels, Biochem. Biophys. Res. Commun. 364 (2007) 429–435.

[27] H.I. Ingólfsson, R.E. Koeppe II, O.S. Andersen, Effects of green tea catechins on gramicidin channel function and inferred changes in bilayer properties, FEBS Lett. 585 (2011) 3101–3105.

[28] S. Adachi, T. Nagao, H.I. Ingólfsson, F.R. Maxfield, O.S. Andersen, L. Kopelovich, I.B. Weinstein, The inhibitory effect of (−)-epigallocatechin gallate on activation of the epidermal growth factor receptor is associated with altered lipid order in HT29 colon cancer cells, Cancer Res. 67 (2007) 6493–6501.

[29] T. Nakayama, T. Hashimoto, K. Kajiya, S. Kumazawa, Affinity of polyphenols for lipid bilayers, Biofactors 13 (2000) 147–151.

[30] T. Hashimoto, S. Kumazawa, F. Nanjo, Y. Hara, T. Nakayama, Interaction of tea catechins with lipid bilayers investigated with liposome systems, Biosci. Biotechnol. Biochem. 63 (1999) 2252–2255.

[31] Y. Tamba, S. Ohba, M. Kubota, H. Yoshioka, H. Yoshioka, M. Yamazaki, Single GUV method reveals interaction of tea catechin (−)-epigallocatechin gallate with lipid membranes, Biophys. J. 92 (2007) 3178–3194.

[32] Y. Sun, W.-C. Hung, F.-Y. Chen, C.-C. Lee, H.W. Huang, Interaction of tea catechin (−)-epigallocatechin gallate with lipid bilayers, Biophys. J. 96 (2009) 1026–1035.

[33] N. Caturla, E. Vera-Samper, J. Villalain, R. Mateo, V. Micol, The relationship between the antioxidant and the antibacterial properties of galloylated catechins and the structure of phospholipid model membranes, Free Radic. Biol. Med. 34 (2003) 648–662.

[34] Y. Uekusa, M. Kamihira, T. Nakayama, Dynamic behavior of tea catechins interacting with lipid membranes as determined by NMR spectroscopy, J. Agric. Food Chem. 55 (2007) 9986–9992.

[35] C.J.F. Böttcher, C.M. Van Gent, C. Pries, A rapid and sensitive sub-micro phosphorus determination, Anal. Chim. Acta. 24 (1961) 203–204.

[36] J.A. Teruel, A. Ortiz, F.J. Aranda, Influence of organotin compounds on phosphatidylserine membranes, Appl. Organomet. Chem. 18 (2004) 111–116.

[37] G. Pabst, M. Rappolt, H. Amenitsch, P. Laggner, Structural information from multilamellar liposomes at full hydration: full q-range fitting with high quality X-ray data, Phys. Rev. E. 62 (2000) 4000–4009.

[38] G. Pabst, R. Koschuch, B. Pozo-Navas, M. Rappolt, K. Lohner, P. Laggner, Structural analysis of weakly ordered membranes stacks, J. Appl. Crystallogr. 63 (2003) 378–1388.

[39] G. Pabst, Global properties of biomimetic membranes: perspectives on molecular features, Biophys. Rev. Lett. 1 (2006) 57–84.

[40] L. Schrödinger, L. Schrödinger, The PyMOL Molecular Graphics System, Version 1.5.0.1, http://www.pymol.org 2010.

[41] A.W. Schüttelkopf, D.M.F. van Aalten, PRODRG: a tool for high-throughput crystallography of protein–ligand complexes, Acta Crystallogr. D Biol. Crystallogr. 60 (2004) 1355–1363.

[42] W.F. Gunsteren, S.R. van Billeter, A.A. Eising, P.H. Hünenberger, P. Krüger, A.E. Mark, W.R.P. Scott, I.G. Tironini, Biomolecular Simulation: The GROMOS96 Manual and User Guide (Zürich, Switzerland), 1996.

[43] A.A. Granovsky, Firefly version 8.0.0, http://classic.chem.msu.su/gran/firefly/index.html.

[44] M.W. Schmidt, K.K. Baldridge, J.A. Boatz, S.T. Elbert, M.S. Gordon, J.H. Jensen, S. Koseki, N. Matsunaga, K.A. Nguyen, S. Su, T.L. Windus, M. Dupuis, J.A. Montgomery Jr., General atomic and molecular electronic structure system, J. Comput. Chem. 14 (1993) 1347–1363.

[45] J. Wong-Ekkabut, M.S. Miettinen, C. Dias, M. Karttunen, Static charges cannot drive a continuous flow of water molecules through a carbon nanotube, Nat. Nanotechnol. 5 (2010) 555–557.

[46] S.-W. Chiu, S.A. Pandit, H.L. Scott, E. Jakobsson, An improved united atom force field for simulation of mixed lipid bilayers, J. Phys. Chem. B 113 (2009) 2748–2763.

[47] H.J.C Berendsen, J.P.M Postma, W.F van Gunsteren, J. Hermans, in: B. Pullman (Ed.), Intermolecular forces, D. Reidel, Dordrecht, The Netherlands, 1981, pp. 331–342.

[48] S. Pronk, S. Páll, R. Schulz, P. Larsson, P. Bjelkmar, R. Apostolov, M.R. Shirts, J.C. Smith, P.M. Kasson, D. van der Spoel, B. Hess, E. Lindahl, GROMACS 4.5: a high-throughput and highly parallel open source molecular simulation toolkit, Bioinformatics 29 (2013) 845–854.

[49] H.J.C. Berendsen, J.P.M. Postma, W.F. van Gunsteren, A. DiNola, J.R. Haak, Molecular dynamics with coupling to an external bath, J. Chem. Phys. 81 (1984) 3684.

[50] S. Miyamoto, P.A. Kollman, Settle: an analytical version of the SHAKE and RATTLE algorithm for rigid water models, J. Comput. Chem. 13 (1992) 952–962.

[51] B. Hess, H. Bekker, H.J.C. Berendsen, J.G.E.M. Fraaije, LINCS: a linear constraint solver for molecular simulations, J. Comput. Chem. 18 (1997) 1463–1472.

[52] U. Essmann, L. Perera, M.L. Berkowitz, T. Darden, H. Lee, L.G. Pedersen, A smooth particle mesh Ewald method, J. Chem. Phys. 103 (1995) 8577.

[53] J. Repáková, P. Čapková, J.M. Holopainen, I. Vattulainen, J. Repa, Distribution, orientation, and dynamics of DPH probes in DPPC bilayer, J. Phys. Chem. B 108 (2004) 13438–13448.

[54] J. Repáková, J.M. Holopainen, M.R. Morrow, M.C. McDonald, P. Capková, I. Vattulainen, Influence of DPH on the structure and dynamics of a DPPC bilayer, Biophys. J. 88 (2005) 3398–3410.

[55] K. Kiwiel, K. Murty, Convergence of the steepest descent method for minimizing quasiconvex functions, J. Optim. Theory Appl. 89 (1996) 221–226.

[56] W. Humphrey, A. Dalke, K. Schulten, VMD — visual molecular dynamics, J. Mol. Graph. 14 (1996) 33–38.

[57] G. Cecv, D. Marsh, Phospholipid Bilayers, Wiley-Interscience, New York, 1993.

[58] J.J. Chicano, A. Ortiz, J.A. Teruel, F.J. Aranda, Organotin compounds alter the physical organization of phosphatidylcholine membranes, Biochim. Biophys. Acta 1510 (2001) 330–341.

[59] V. Luzzati, in: D. Chapman (Ed.), Biological Membranes, Academic Press, New York, 1968, pp. 71–123.

[60] A. Pérez-Lara, A. Ausili, F.J. Aranda, A. de Godos, A. Torrecillas, S. Corbalán-García, J.C. Gómez-Fernández, Curcumin disorders 1,2-dipalmitoyl-sn-glycero-3-phosphocholine membranes and favors the formation of nonlamellar structures by 1,2-dielaidoyl-sn-glycero-3-phosphoethanolamine, J. Phys. Chem. B 114 (2010) 9778–9786.

[61] S. Berenyi, J. Mihaly, S. Kristyan, L. Naszalyi Nagy, J. Telegdi, A. Bota, Thermotropic and structural effects of poly(malic acid) on fully hydrated multilamellar DPPC–water systems, Biochim. Biophys. Acta 1828 (2013) 661–669.

[62] A. Tardieu, V. Luzzati, F.C. Reman, Structure and polymorphism of the hydrocarbon chains of lipids: a study of lecithin–water phases, J. Mol. Biol. 75 (1973) 711–733.

[63] K. Lohner, A. Latal, G. Degovics, P. Garidel, Packing characteristics of a model system mimicking cytoplasmic bacterial membranes, Chem. Phys. Lipids 111 (2001) 177–192.

[64] A. Ortiz, J.A. Teruel, M.J. Espuny, A. Marqués, A. Manresa, F.J. Aranda, Interactions of a Rhodococcus sp. biosurfactant trehalose lipid with phosphatidylethanolamine membranes, Biochim. Biophys. Acta 1778 (2008) 2806–2813.

[65] J.T. Kim, J. Mattai, G.G. Shipley, Bilayer interactions of ether- and ester-linked phospholipids: dihexadecyl- and dipalmitoylphosphatidylcholines, Biochemistry 26 (1987) 6599–6603.

[66] C. Huang, T.J. McIntosh, Probing the ethanol-induced chain interdigitations in gel-state bilayers of mixed-chain phosphatidylcholines, Biophys. J. 72 (1997) 2702–2709.

[67] G. Pabst, S. Danner, S. Karmakar, G. Deutsch, V.A. Raghunathan, On the propensity of phosphatidylglycerols to form interdigitated phases, Biophys. J. 93 (2007) 513–525.

[68] D.G. Nagle, D. Ferreira, Y.D. Zhou, Epigalloca techin-3-gallate (EGCG): chemical and biomedical perspectives, Phytochemistry 67 (2006) 1849–1855.

[69] S.K. Patra, F. Rizzi, A. Silva, D.O. Rugina, S. Bettuzzi, Molecular targets of (−)-epigallocatechin-3-gallate (EGCG): specificity and interaction with membrane lipid rafts, J. Physiol. Pharmacol. 59 (2008) 217–235.

[70] O.S. Andersen, R.E. Koeppe II, Bilayer thickness and membrane protein function: an energetic perspective, Annu. Rev. Biophys. Biomol. Struct. 36 (2007) 107–130.

[71] Y.-P. Zhang, R.N.A.H. Lewis, R.N. McElhaney, Calorimetric and spectroscopic studies of the thermotropic phase behaviour of the n-saturated 1,2-diacylphosphatidylglycerols, Biophys. J. 72 (1997) 779–793.

[72] A. Blume, W. Hübner, G. Messner, Fourier transform infrared spectroscopy of ¹³C=O-labeled phospholipids hydrogen bonding to carbonyl groups, Biochemistry 27 (1988) 8239–8249.

[73] M. Kranenburg, M. Vlaar, B. Smit, Simulating induced interdigitation in membranes, Biophys. J. 87 (2004) 1596–1605.

[74] A.S. Ulrich, F. Volke, A. Watts, The dependence of phospholipids head-group mobility on hydration as studied by deuterium-NMR spin-lattice relaxation time measurements, Chem. Phys. Lipids 55 (1990) 64–66.

[75] K.G. Chen, J.C. Valencia, B. Lai, G. Zhang, J.K. Paterson, F. Rouzaud, W. Berens, S.M. Wincovitch, S.H. Garfield, R.D. Leapman, V.J. Hearing, M.M. Gottesman, Melanosomal sequestration of cytotoxic drugs contributes to the intractability of malignant melanomas, Proc. Natl. Acad. Sci. U. S. A. 103 (2006) 9903–9907.

[76] L. Sánchez-del-Campo, M.F. Montenegro, J. Cabezas-Herrera, J.N. Rodríguez-López, The critical role of alpha-folate receptor in the resistance of melanoma to methotrexate, Pigment Cell Melanoma Res. 22 (2009) 588–600.

[77] T. Xie, T. Nguyen, M. Hupe, M.L. Wei, Multidrug resistance decreases with mutations of melanosomal regulatory genes, Cancer Res. 69 (2009) 992–999.

[78] Z.M. Huang, M. Chinen, P.J. Chang, T. Xie, L. Zhong, S. DemetriouS, M.P. Patel, R. Scherzer, E.V. Sviderskaya, D.C. Bennett, G.L. Millhauser, D.H. Oh, J.E. Cleaver, M.L. Wei, Targeting protein-trafficking pathways alters melanoma treatment sensitivity, Proc. Natl. Acad. Sci. U. S. A. 109 (2012) 553–558.

[79] M.P. Fernández-Pérez, M.F. Montenegro, M. Sáez-Ayala, L. Sánchez-del-Campo, A. Piñero-Madrona, J. Cabezas-Herrera, J.N. Rodríguez-López, Suppression of antifolate resistance by targeting the myosin Va trafficking pathway in melanoma, Neoplasia 15 (2013) 826–839.